Quenching and Annealing of Zone-Refined Aluminum*

M. DOYAMA† AND J. S. KOEHLER
Department of Physics, University of Illinois, Urbana, Illinois
(Received 14 October 1963; revised manuscript received 13 December 1963)

Detailed annealing studies have been done on quenched zone-refined aluminum. The research was undertaken to determine the migration energy of the divacancy $E_M{}^2$ and the binding energy of the divacancy B_2 in pure aluminum. It was found that $E_M{}^2=0.50\pm0.04$ eV and $B_2=0.17\pm0.05$ eV. Some discussion of the properties of larger vacancy clusters is given.

I. INTRODUCTION

DURING the last several years an appreciable amount of information concerning point defects has been obtained both from equilibrium and nonequilibrium measurements. When metals are quenched from a high temperature to a low temperature, most of the imperfections present in thermal equilibrium at the high temperature can be frozen in. In close-packed metals the dominant imperfections are vacancies, vacancy clusters, and dislocations arising from collapsed vacancy clusters.

The equilibrium measurements in aluminum have been made by Simmons and Balluffi.[1] The thermal quenching in aluminum has been done by Bradshaw and Pearson,[2] Panseri and Federighi,[3] and DeSorbo and Turnbull.[4] They give the energy required to form a vacancy E_F to be 0.77 ± 0.03 eV. Simmons *et al.*[5] give the electrical resistivity due to 1% vacancies as $(2.2\pm0.7)\times10^{-6}$ ohm-cm. Takamura[6] quenched aluminum and studied the volume change due to the quenching.

Desorbo and Turnbull[4] measured the activation energy of motion of a vacancy, $E_F=0.65\pm0.06$ eV, by quenching a zone-refined aluminum specimen (residual resistivity ratio $\alpha=R\,273°K/R\,4.3°K=4200$) from below 300°C, therefore avoiding divacancy formation. They also measured $E_M=0.52\pm0.04$ eV for a less pure aluminum specimen ($\alpha=800$) by quenching from 332°C. DeSorbo and Turnbull emphasized the effect of impurity atoms on the activation energy for motion of the defects. Panseri and Federighi found E_M, from two isochronal annealing curves, to be between 0.37 and 0.58 eV.

Lundy and Murdock[7] measured the activation energy for self-diffusion in aluminum and found E_D to be 1.46 eV. In recent years a number of direct observations on the behavior of the annealing of the quenched-in vacancies in aluminum have been made with electron microscopes.[8–13]

Some measurements have been made to determine the properties of divacancies in silver[14] and gold.[15,16] Theoretical calculations on annealing have been done by Dienes and Damask, and Koehler, de Jong, and Seitz.[15–17]

The present research is aimed at determining the activation energy for motion of a divacancy and the binding energy of a divacancy as well as investigating the binding energy of larger clusters in aluminum.

II. EXPERIMENTAL PROCEDURE

The specimen material for this experiment was AIAG 99.9999% pure zone-refined aluminum. The impurities in the zone-refined aluminum ingot were as follows: Si not detected, Fe 0.3 ppm, and Cu 0.3 ppm. The elements sought, but not detected, were Ti, Zn, Ba, and Co. This aluminum was drawn into a wire of 1 mm in diameter by AIAG. We then drew the wires to 22 mils and smaller using diamond dies. The wire was etched with a hot mixture of 95% phosphoric acid and 5% nitric acid after each drawing. A 22-mil-diam wire was mounted on a frame and 5-mil zone-refined aluminum lead wires, 10 cm apart, were spot-welded to the specimen. The residual resistivity after an anneal was about 8×10^{-10} ohm-cm. The specimen was heated by passing a direct current through it and quenched by plunging the frame into an eutectic mixture of $CaCl_2$ and water kept at −40°C.

The change in temperature during a quench was ob-

* Supported in part by the U. S. Army Research Office (Durham).
† Present address: Argonne National Laboratory, Argonne, Illinois.
[1] R. O. Simmons and R. W. Balluffi, Phys. Rev. **117**, 52 (1960).
[2] F. J. Bradshaw and S. Pearson, Phil. Mag. **2**, 570 (1957).
[3] C. Panseri and T. Federighi, Phil. Mag. **3**, 1223 (1958).
[4] W. DeSorbo and D. Turnbull, Acta Met. **7**, 83 (1959); Phys. Rev. **115**, 560 (1959).
[5] R. O. Simmons, J. S. Koehler, and R. W. Balluffi, *Symposium on Radiation Damage in Solids and Reactor Materials, Venice, 1962; Radiation Damage in Solids I* (International Atomic Energy Agency, Vienna), p. 155.
[6] J. Takamura, Metal Phys. **2**, 112 (1956).
[7] T. S. Lundy and J. F. Murdock, J. Appl. Phys. **33**, 1671 (1962).
[8] P. B. Hirsch, J. Silcox, R. E. Smallman, and K. H. Westmacott, Phil. Mag. **3**, 897 (1958).
[9] J. Silcox and M. J. Whelan, Phys. Mag. **5**, 1 (1960).
[10] D. Kuhlman-Wilsdorf and H. G. F. Wilsdorf, J. Appl. Phys. **31**, 516 (1960).
[11] S. Yoshida, J. Shimomura, and M. Kiritani, J. Phys. Soc. Japan **17**, 1196 (1962).
[12] S. Yoshida, M. Kiritani, and Y. Shimomura, J. Phys. Soc. Japan **18**, 175 (1963).
[13] R. M. J. Cotterill and R. L. Segall, Phil. Mag. **8**, 1105 (1963).
[14] M. Doyama and J. S. Koehler, Phys. Rev. **127**, 21 (1962).
[15] M. de Jong and J. S. Koehler, Phys. Rev. **129**, 49 (1963); **129**, 49 (1963).
[16] J. S. Koehler, M. de Jong, and F. Seitz, J. Phys. Soc. Japan **18**, Suppl. III, 1 (1963).
[17] G. J. Dienes and A. C. Damask, Discussions Faraday Soc. **31**, 29 (1961); A. C. Damask, G. J. Dienes, and V. G. Weizer, Phys. Rev. **113**, 781 (1959).

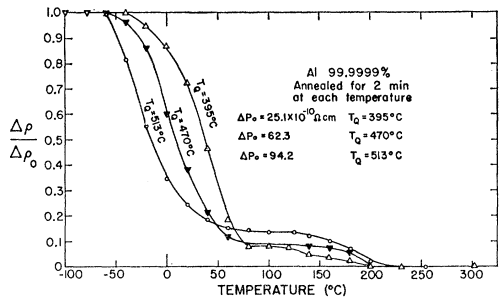

FIG. 1. Isochronal annealing curves; $\Delta\rho/\Delta\rho_0$ versus annealing temperature. The specimen was annealed for 2 min at temperatures 20°C apart.

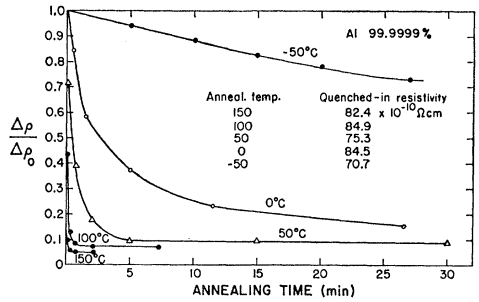

FIG. 2. Isothermal annealing curves at 150, 100, 50, 0, and −50°C. The quench temperature was near 500°C. The quenched-in resistivity was shown.

served on an oscilloscope and photographed using a Polaroid camera. The rate of cooling remained nearly constant until the temperature of the specimen approached that of the quenching medium. The constant cooling rate was 1.4×10^4 °C/sec. Specimens were annealed in a constant temperature bath consisting either of alcohol saturated with Al_2O_3 (to prevent dissolving specimens) or silicone oil.

The resistance of the specimen was measured while it was immersed in liquid helium. To determine the current through the specimen, a Rubicon one-hundredth ohm standard resistance was connected in series with the specimen. The voltage across the standard resistance was measured with a Leeds and Northrup type K-2 potentiometer. The voltage across the lead wires was measured by a Rubicon thermofree microvolt potentiometer in conjunction with a Rubicon photoelectric galvanometer.

Some specimens were mounted on a mica frame, heated in a furnace, and quenched into a eutectic mixture of $CaCl_2$ and water kept at −40°C.

The resistivity of pure aluminum at 20.0°C was taken to be 2.6548 μohm-cm.[18]

III. EXPERIMENTAL RESULTS

A. Isochronal Annealing

A specimen was quenched from 513, 470, and 395°C, and was annealed for two-minute intervals at temperatures 20°C apart. Isochronal annealing curves are shown in Fig. 1.

Figure 1 shows that there exist two separate annealing stages. Stage I, which corresponds to the first stage of Panseri and Federighi,[3] is found near 0°C. Its temperature T_1 is highly dependent upon the quench temperature T_Q in the following manner: As T_Q is increased, T_1 decreases. Our value of T_1 for a zone-refined aluminum specimen is lower than the value reported by Panseri and Federighi for their low-purity aluminum specimen.[3] Stage II, which corresponds to the second stage of Panseri and Federighi, is observed near 190°C and is in agreement with Panseri and Federighi. A plateau is observed between the two stages. The value of the fraction $\Delta\rho/\Delta\rho_0$ after the completion of stage I is larger for higher values of the quench temperature.

B. Isothermal Annealing

When a specimen is quenched from temperature T_Q, the electrical resistivity increases by $\Delta\rho_0$. When this quenched specimen is annealed at a temperature T_A, some of the quenched-in resistivity can be annealed out, leaving a quenched-in resistivity $\Delta\rho_R$. This remaining resistivity $\Delta\rho_R$ can be annealed out near 200°C.

The first of three specimens was quenched from near 500°C and was annealed at −50, 0, 50, 100, and 150°C. The annealing curves are given in Fig. 2. The time required to anneal out $\frac{1}{2}(\Delta\rho_0-\Delta\rho_R)$ is given in Table I.

TABLE I. Influence of concentration and annealing temperature on the annealing rate of pure aluminum.

No.	Specimen No.	$\Delta\rho_0$	T_A	$\tau_{1/2}$	Initial rate of annealing	n_1[a]	n_2[a]
1	AL-AIAG-4	8.24×10^{-10} ohm-cm	150°C	<2 sec	...		
2	4	84.9	100	≃3 sec	1×10^{-9} ohm-cm/sec	3.3×10^5	3.3×10^7
3	4	75.3	50	24 sec	1.687×10^{-10}	1.36×10^5	2.2×10^7
4	4	84.5	0	2½ min	4.96×10^{-11}	8.48×10^3	5.45×10^6
5	4	70.7	−50	45 min	1.36×10^{-12}	2.5×10^2	8.78×10^5
6	1	131.2	−50	17¾ min		9.84×10	3.46×10^5
7	1	90.67	−50	25 min		1.385×10^2	4.87×10^5
8	4	2.71	25	31 min		1.12×10^6	3.82×10^8
9	3	15.43	25	24 min		8.64×10^5	2.95×10^8
10	3	62.64	25	2.4 min		8.64×10^4	2.95×10^7

[a] n_1 is the number of jumps that a single vacancy makes during $\tau_{1/2}$, and n_2 is the number of jumps that a divacancy makes during $\tau_{1/2}$.

[18] C. S. Taylor, L. A. Willey, D. W. S. Smith, and J. D. Edwards, Metals and Alloys **9**, 189 (1938).

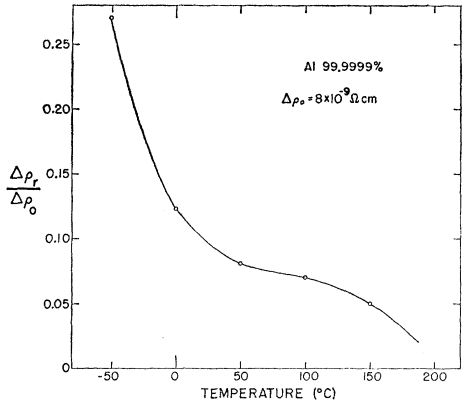

FIG. 3. The ratio $\Delta\rho_r/\Delta\rho_0$ of the remaining resistivity $\Delta\rho_r$ and $\Delta\rho_0$ versus annealing temperature.

$\Delta\rho_R$ versus the annealing temperature T_A is plotted in Fig. 3. The quenched specimen was annealed for a long time at temperature T_A, and then was annealed isochronally for two minutes at temperatures 20°C apart

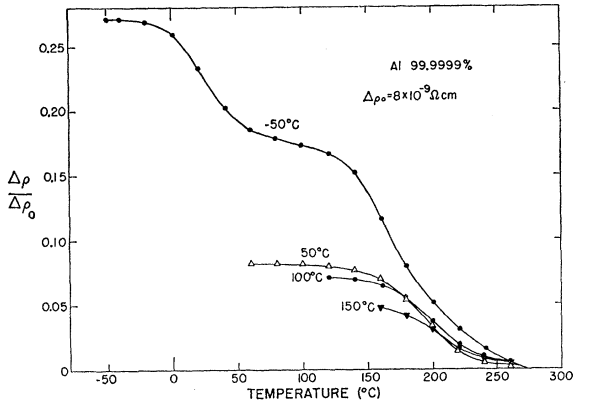

FIG. 4. Isochronal annealing curves of the remaining resistivity. The ratio $\Delta\rho/\Delta\rho_0$ versus annealing temperature was plotted. $\Delta\rho$ is the resistivity after each anneal. $\Delta\rho_0$ is the quenched-in resistivity. Quench temperature was near 500°C.

(see Fig. 4). A second specimen was quenched from 500 and 595°C and annealed at −50.0°C (Fig. 5). A third specimen was quenched from 300, 374, and 452°C, and annealed at 25.0°C (Fig. 6).

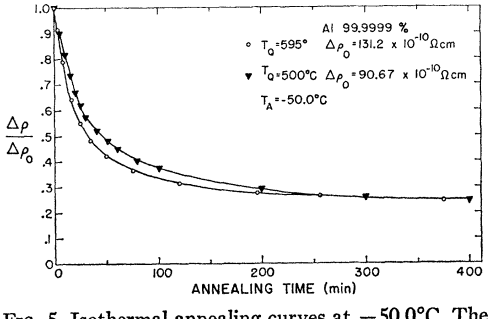

FIG. 5. Isothermal annealing curves at −50.0°C. The specimen was quenched from 500 and 595°C.

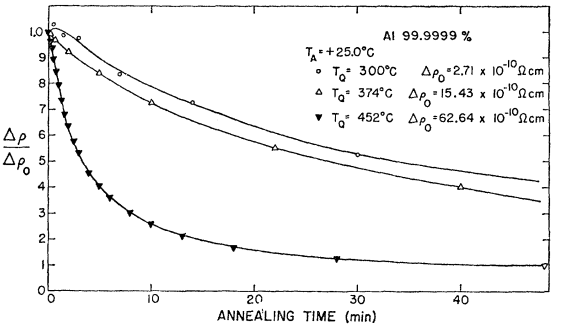

FIG. 6. Isothermal annealing curves at 25.0°C. The specimen was quenched from 300, 374, and 452°C.

IV. DISCUSSION AND INTERPRETATION

A. Annealing at −50°C and E_M for a Divacancy

The data described in Figs. 2, 5, 7, 8, 9, and 12 can be used to obtain information concerning the energy of migration and the binding energy of divacancies. Consider the annealing at −50 and −60°C following a quench from 538°C (Fig. 7). Immediately after the quench, one should have only single vacancies and divacancies since not enough time has elapsed to allow larger clusters to form. At such low temperatures the vacancies are very sluggish. At −50°C a single vacancy ($E_M{}^V$=0.68 eV) makes only 0.78 atomic jumps per second, whereas a divacancy makes 516 jumps per second if $E_M{}^2$=0.50 eV. The low observed activation energy (0.50±0.04 eV) is therefore interpreted to be that for the motion of a divacancy. Further evidence supporting this assignment will be given below. The number of jumps made during the half-time (45 min at −50°C after a 500°C quench) are 2.1×10^3 for single vacancies and 1.39×10^6 for divacancies. The quenched-in resistivity change of 7.1×10^{-9} ohm-cm corresponds to an initial vacancy concentration of 3.2×10^{-5}. The number of jumps made by a divacancy is reasonable if

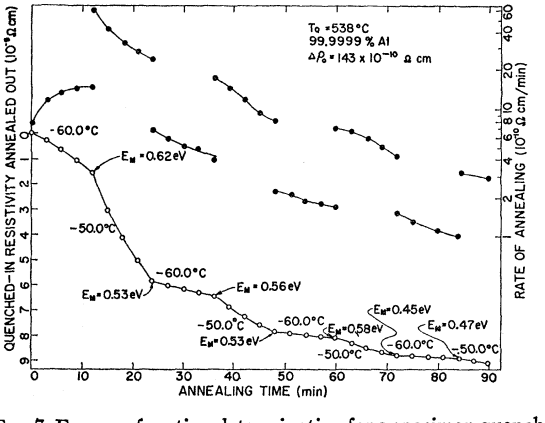

FIG. 7. Energy of motion determination for a specimen quenched from 538°C and annealed at −50.0 and −60.0°C. Defect resistivity and rate of annealing versus annealing time were plotted. Solid dots give rates of annealing.

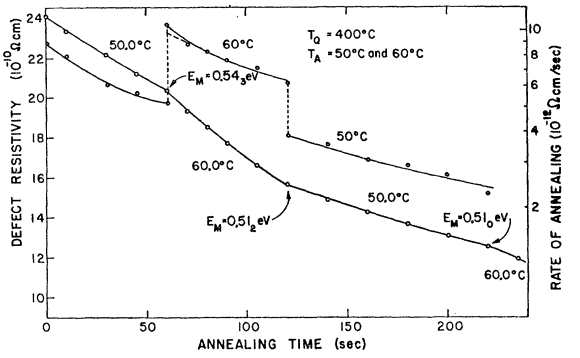

FIG. 8. Energy of motion determination for a specimen quenched from 400°C and annealed at 50.0 and 60.0°C. Defect resistivity and annealing rate versus annealing time were plotted.

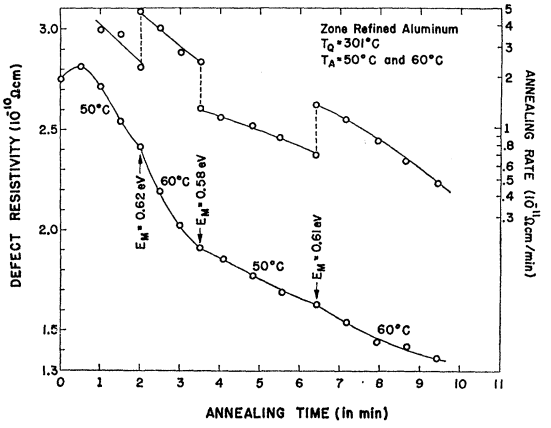

FIG. 9. Energy of motion determination for a specimen quenched from 301°C and annealed at 50.0 and 60.0°C. Defect resistivity and annealing rate versus annealing time were plotted.

we assume divacancies disappear at dislocations. Note that this interpretation requires that an appreciable number of divacancies are formed during a quench from 500°C or above.

B. Binding Energy for a Divacancy in Aluminum

The binding energy of divacancies in aluminum is expected to be a larger fraction of the formation energy of a single vacancy than is observed in gold. The experimental findings which support this suggestion are as follows:

(1) A specimen quenched from 400°C and annealed at 50 and 60°C yield a migration energy of 0.52 eV (Fig. 8). It is only when the quenching temperature is quite low (301°C) that the migration energy obtained on cycling from 50 to 60°C and back begins to rise (E_M=0.60 eV) and approach a value appropriate for a single vacancy (Fig. 9).

(2) When a specimen is quenched from above 500°C, the appreciable annealing which occurs at −50°C indicates that an appreciable divacancy concentration is produced during the quench.

Let us therefore examine experimental methods available which can determine the binding energy B_2 of the divacancy. They are:

(1) The apparent activation energy for the motion of defects at various annealing temperatures and various defect concentrations.

(2) Measurement of the annealing temperature T_1 above which clusters of defects do not form at various defect concentrations. During annealing at temperatures above T_1, a divacancy breaks up before it encounters another defect.

1. *The Apparent Activation Energy for Motion of Defects*

Let us consider a specimen containing a mixture of single vacancies and divacancies. If an equilibrium between the single vacancies and divacancies is achieved, the effective diffusion constant is given by[15]

$$D=\nu_1 a^2 \exp\left(-\frac{E_M{}^1}{kT}\right) \times\left[\frac{1+3(\nu_2/\nu_1)c_1\exp[(E_M{}^1+B_2-E_M{}^2)/kT]}{1+24c_1\exp(B_2/kT)}\right], \quad (1)$$

where ν_1 and ν_2 are the frequency factors of a single vacancy and a divacancy, respectively. a is the closest distance between atoms $E_M{}^1$ and $E_M{}^2$ are the activation energies for motion of a single and of a divacancy respectively, and c_1 is the fractional concentration of single vacancies. When a quenched specimen is annealed at temperature T_1 and its annealing temperature is changed to T_2, the apparent activation energy for motion of the defects $E_M{}^A$ is given by

$$E_A=\frac{kT_1T_2}{T_2-T_1}\ln\left[\frac{\text{rate}(T_2)}{\text{rate}(T_1)}\right]=\frac{kT_1T_2}{T_2-T_1}\ln\frac{D(T_2)}{D(T_1)}=\frac{kT_1T_2}{T_2-T_1} \times\ln\left[\frac{\exp(-E_M{}^1/kT_2)\{1+3(\nu_2/\nu_1)c_1\exp[(E_M{}^1+B_2-E_M{}^2)/kT_2]\}\{1+24c_1\exp(B_2/kT_1)\}}{\exp(-E_M{}^1/kT_1)\{1+3(\nu_2/\nu_1)c_1\exp[(E_M{}^1+B_2-E_M{}^2)/kT_1]\}\{1+24c_1\exp(B_2/kT_2)\}}\right]. \quad (2)$$

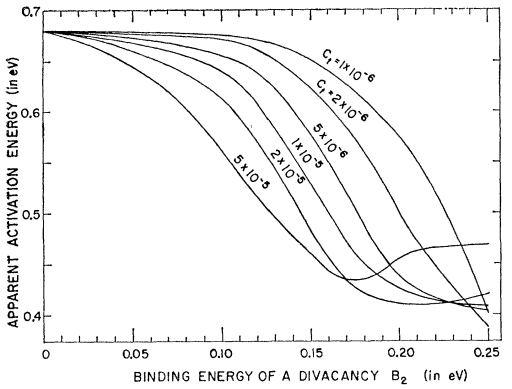

FIG. 10. Apparent activation energy versus binding energy of a divacancy at various fractional concentrations of total defects $c_t=c_1+2c_2$.

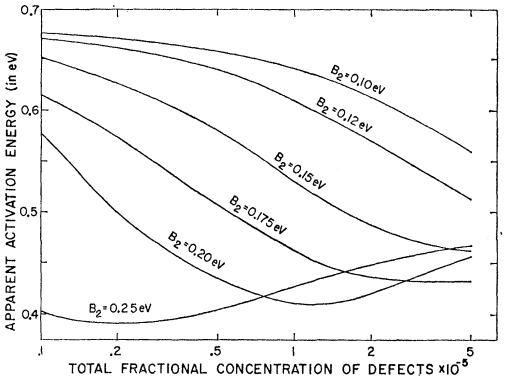

FIG. 11. Apparent activation energy versus total concentration of defects $c_t=c_1+2c_2$ at various binding energies of a divacancy.

Figure 10 gives the relationship between the binding energy of a divacancy and the apparent activation energy E_A for the annealing of a mixture of defects, assuming that single vacancies and the divacancies are in thermal equilibrium. The annealing temperatures were taken to be 60 and 50°C. The total defect concentration $c_t=c_1+2c_2$. Figure 11 gives the relationship between the apparent activation energy for motion of the defects and the total concentration c_t upon annealing at 50 and 60°C. Equation (2) gives $E_M=E_M{}^1$ when $12c_t\exp(B_2/kT)\ll1$, and $E_A\cong E_M{}^2$ when

$$12c_t\exp(B_2/kT)\gg1.$$

A specimen was quenched from 400°C ($\Delta\rho_0=2.4\times10^{-9}$ ohm-cm) and annealed at 50.0 and 60.0°C (Fig. 8). The apparent activation energy for motion of the defects was calculated to be 0.52 eV. One obtains $B_2=0.16\pm0.02$ eV by finding the point on Fig. 11 which corresponds to an apparent activation energy of 0.52 eV and $c_t=7\times10^{-6}$ which corresponds to a value of $\Delta\rho=1.57\times10^{-9}$ ohm-cm.

Another specimen was quenched from 301°C ($\Delta\rho_0=3.75\times10^{-10}$ ohm-cm) and annealed at 50.0 and 60.0°C (Fig. 9). The average value of the apparent activation energy for motion of the defects was calculated to be 0.61 eV at the average value of $c_t=1\times10^{-6}$. B_2 is found to be 0.18 ± 0.03 eV in the manner mentioned above.

In some cases the apparent activation energy is smaller than either $E_M{}^1$ or $E_M{}^2$.[14] Differentiating Eq. (2), the minimum apparent energy for motion of the defects is obtained when the concentration is given by solutions of

$$+72c_1{}^2\frac{\nu_2}{\nu_1}\Big[+24\exp\frac{B_2}{k}\Big(\frac{1}{T_2}+\frac{1}{T_1}\Big)\Big\{\exp\frac{E}{kT_2}-\exp\frac{E}{kT_1}\Big\}-\frac{3\nu_2}{\nu_1}\exp\frac{E}{k}\Big(\frac{1}{T_2}+\frac{1}{T_1}\Big)\Big\{\exp\frac{B_2}{kT_2}-\exp\frac{B_2}{kT_1}\Big\}\Big]$$

$$+72\frac{c_1\nu_2}{\nu_1}\Big[+\Big\{\exp\frac{B_2}{kT_2}+\exp\frac{B_2}{kT_1}\Big\}\Big\{\exp\frac{E}{kT_2}-\exp\frac{E}{kT_1}\Big\}-\Big\{\exp\frac{B_2}{kT_2}-\exp\frac{B_2}{kT_1}\Big\}\Big\{\exp\frac{E}{kT_2}+\exp\frac{E}{kT_1}\Big\}\Big]$$

$$+\frac{3\nu_2}{\nu_1}\Big\{\exp\frac{E}{kT_2}-\exp\frac{E}{kT_1}\Big\}-24\Big\{\exp\frac{B_2}{kT_2}-\exp\frac{B_2}{kT_1}\Big\}=0, \quad (3)$$

where E is $E_M{}^1+B_2-E_M{}^2$. A specimen was quenched from 504°C and was annealed at 50.0 and 60.0°C (Fig. 12). The apparent activation energy for motion was found to be 0.46 eV. This is lower than the activation energy for motion of a divacancy and happens when $3(\nu_2/\nu_1)c_1\exp[(E_M{}^1+B_2-E_M{}^2)/(kT)]\gg1$ and $24c_1\exp(B_2/kT)\ll1$. Figures 10 and 11 also show this low activation energy.

The above discussion is valid only when the characteristic time τ_c to achieve equilibrium between single vacancies and divacancies is much shorter than the annealing half-time, where τ_c is given by[15]

$$\tau_c{}^{-1}=7\nu_1\Big\{1+48c_t\exp\Big(\frac{B_2}{kT}\Big)\Big\}^{1/2}\exp\Big(-\frac{E_M{}^1+B_2}{kT}\Big). \quad (4)$$

Choosing $\nu_1=10^{13}$, $c_t=3\times10^{-5}$, $T=50$°C, and $B_2=0.2$/eV, then $\tau_c=0.6$ sec. The observed half-time of annealing in this case was 24 sec, which is much longer than τ_c at this temperature. This argument cannot be used on the data in Fig. 7 because there the critical time is 36 h which is much longer than the annealing half-time.

2. Initial Annealing Rate and Half-Time of Annealing

In an isothermal annealing, when a specimen is quenched each time from the same temperature and is annealed at various temperatures, it is expected that the initial divacancy to single-vacancy concentration ratio c_{20}/c_{10} is the same after each quench as long as the quench speed remains the same. If the divacancies break up during the annealing process, we expect the annealing rate to be slower than that seen when the divacancies do not break up. Thus, at a temperature where the breakup of divacancies becomes appreciable, the half-time of annealing becomes longer than the value expected for a lower temperature where no breakup of divacancies occurs.

The electrical resistivity due to single vacancies and divacancies is

$$\Delta\rho = A_1 c_1 + 2(A_1 - \Delta_2) c_2 , \tag{5}$$

$$\frac{d\Delta\rho}{dt} = -\alpha_{11} c_1^2 \Delta_2 + \beta_2 c_2 \Delta_2 - A_1 \delta_1 c_1 - 2(A_1 - \Delta_2)\delta_2 c_2 , \tag{6}$$

where Δ_2 is the change in electrical resistivity when a divacancy is formed from two single vacancies. A_1 is a constant and is 2.2×10^{-4} ohm-cm.[5] If Δ_2 is small and negligible, then

$$\frac{d\Delta\rho}{dt} = -\frac{A_1\nu_1}{n}\left\{12 c_1 \exp\left(-\frac{E_M{}^1}{kT}\right) + 8\frac{\nu_2}{\nu_1} c_2 \exp\left(-\frac{E_M{}^2}{kT}\right)\right\}, \tag{7}$$

where n is the number of jumps that a single vacancy or a divacancy makes before it reaches a sink. ν_1 and ν_2 are the frequency factors for a single vacancy and a divacancy, respectively. $E_M{}^1$ and $E_M{}^2$ are the activation energies for motion of single vacancy and divacancy, respectively. The initial rate of annealing is

$$\left(\frac{d\Delta\rho}{dt}\right)_{t=0} = -\frac{A_1\nu_1 c_{t0}}{n}\left[12\exp\left(-\frac{E_M{}^1}{kT}\right) + 8\frac{c_{20}}{c_{t0}} \times\left\{-3\exp\left(-\frac{E_M{}^1}{kT}\right) + \frac{\nu_2}{\nu_1}\exp\left(-\frac{E_M{}^1}{kT}\right)\right\}\right], \tag{8}$$

where c_{t0} is the total initial void concentration, i.e., $c_{t0} = c_{10} + 2c_{20}$. The first two terms represent the annealing of single vacancies and the third, the annealing of divacancies.

A specimen was quenched from near 500°C and was annealed at −50, 0, 50, 100, and 150°C (Fig. 2). The initial annealing rate above 50°C can be explained by the annealing of single vacancies, that is, the annealing is governed by the first term of Eq. (12), using $n=10^6$, $A_1=2.2\times10^{-4}$ ohm-cm, and $\nu_1=\nu_2=10^{13}$ (Table I).

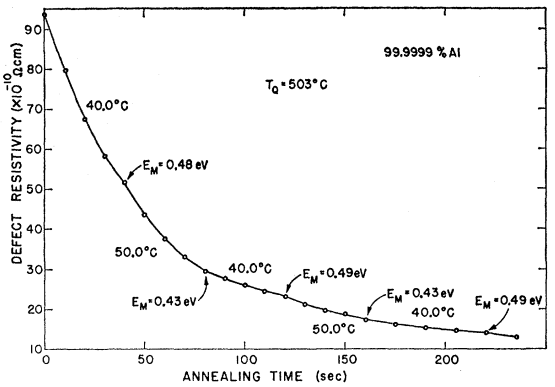

FIG. 12. Energy of motion determination for a specimen quenched from 503°C and annealed at 40.0 and 50.0°C. Defect resistivity and rate of annealing versus annealing time were plotted.

Below 0°C the role of the second term is important. This means that below 0°C the annealing of divacancies plays an important role in the annealing process. If there is an appreciable number of divacancies in a quenched specimen at a temperature 25°C or above, the divacancies must break up before they reach sinks. If there are no divacancies in a quenched specimen, the average time τ_c to form divacancies is 5 sec at 25°C. The time τ_c, in which a divacancy makes 10^6 jumps, is 7 sec. The observed annealing half-time is about 1 min. Therefore, in this case, divacancies must also break up before they reach sinks. The breakup time τ_B of a divacancy is

$$\tau_B = \left\{14\nu\exp\left(-\frac{E_M{}^1 + B_2}{kT}\right)\right\}^{-1}. \tag{9}$$

The time τ for a divacancy to travel n jumps is

$$\tau = \left[\frac{4\nu\exp(-E_M{}^2/kT)}{n}\right]^{-1}, \tag{10}$$

when

$$7n\exp\left(-\frac{E_M{}^1 + B_2 - E_M{}^2}{kT}\right) = 2.$$

Setting $n=10^6$, $T=50$°C, $E_M{}^1=0.68$ eV, and $E_M{}^2=0.50$ eV, one obtains $B_2=0.23$ eV. For $T=-50$°C, $B_2=0.12$. Therefore, the binding energy of a divacancy is estimated to be between 0.12 and 0.23 eV from the initial annealing rate.

Let us examine Table I carefully. The number of jumps that a single vacancy or a divacancy makes before it reaches a sink is of the order of 10^6 in our specimen. Below 0°C, the number of jumps made by a single vacancy during the half-time of annealing is much smaller than 10^6, but the number of jumps a divacancy makes during the half-time of annealing is of the order of 10^6. The divacancies play an important role in the annealing process below 0°C. However, in the annealing above 25°C, the number of jumps that a divacancy makes during the half-time of annealing is more than a

few times 10^7, which is greater than 10^6. The number of jumps that a single vacancy makes during the half-time of annealing is of the order of a few times 10^5. We see that the annealing process of single vacancies is predominant; therefore, above 25°C, a divacancy will break up during the time it travels to a sink. Assuming the number of jumps to a sink is 10^6, one obtains the binding energy of a divacancy to be 0.20 eV.

C. Higher Clusters of Vacancies

The properties and behavior of trivacancies, quadrivacancies, and higher clusters are so little known that it is still difficult to draw any definite conclusions.

Let us examine the data of Fig. 7. If we suppose that only single vacancies and divacancies are mobile and that they combine to form trivacancies, quadrivacancies, and higher clusters, one can show that the predictions of the model do not fit the observed facts as follows:

The equations governing the cluster formation are

$$\begin{aligned} dc_1/dt &= -2\alpha c_1^2 - \beta c_1 c_2 - \delta c_1 c_3, \\ dc_2/dt &= +\alpha c_1^2 - \beta c_1 c_2 - \beta c_2^2, \\ dc_3/dt &= +\beta c_1 c_2 - \delta c_1 c_3, \\ dc_4/dt &= +(\beta/2) c_2^2 + \delta c_1 c_3, \end{aligned} \tag{11}$$

where $\alpha = 84\nu_1 e^{-E_M{}^1/kT}$, $\beta = 20\nu_2 e^{-E_M{}^2/kT}$, and $\delta = \alpha$. If we neglect the term in δ, which is small during the majority of the anneal, the first two equations can be solved by introducing a new variable:

$$z = \alpha - (\beta - 2\alpha)(c_2/c_1). \tag{12}$$

If c_2/c_1 is sufficiently large that z is negative, then one uses instead the negative of the right side as variable. The resulting solutions are

$$\ln\frac{c}{c_{10}} = \frac{\alpha(3\beta-4\alpha)}{(\beta-2\alpha)^2}\ln\frac{z}{z_0} - \frac{\beta}{(\beta-2\alpha)^2}\{z - z_0\}, \tag{13}$$

where c_{10} and z_0 are initial values of c_1 and z. The equation giving the time dependence is

$$\ln z + \frac{\beta}{(\beta-2\alpha)^2}z + \frac{1}{4}\left\{\frac{\beta}{(\beta-2\alpha)^2}\right\}^2 z^2 + \cdots = -c_{10}(\beta-2\alpha)(t-t_0)e^{\alpha\beta/(\beta-2\alpha)^2}, \tag{14}$$

where t_0 is determined by the initial value of z. The variable z is useful because it rapidly tends toward zero. For example, at −50°C using $\nu_1 = 4\nu_2 = 10^{13}$ cps and $E_M{}^1 = 0.65$ eV and $E_M{}^2 = 0.50$ eV, one finds that if $c_2 = 0$ initially then z drops to a tenth its initial value in 2.69 min. z is a hundredth its initial value in 5.37 min. During this period, c_1 drops by less than one percent of its initial value which we took to be 5.80×10^{-5}. Note that in the steady state the ratio c_2/c_1 is a constant. This trend toward the constant value $(\alpha/\beta - 2\alpha)$ occurs also if the initial value of c_2/c_1 is high. For example, if initially $c_2/c_1 = 0.10$ at −50°C, then in 2.06 min $c_1 = 0.90c_{10}$ and $c_2/c_1 = 0.0272$. After 19.59 min, $c_1 = 0.80c_{10}$ and $-z = 5.74\times10^{-6}$ so that $c_2/c_1 = 6.9309\times10^{-3}$ which is the steady-state value. If one starts at −50°C with $c_2 = 0$ and $c_1 = c_{10} = 5.8\times10^{-5}$, the time required to anneal out half the vacancies is 391 min. If instead one starts with $c_2/c_1 = 0.10$ and $c_1 = 5.80\times10^{-5}$, the time required to anneal out half of the vacancies is 36.94 min. Note that the initial value $c_2/c_1 = 0.10$ is much too large.

The steady-state concentration of divacancies achieved at −50°C is much too small to fit the effective energy of migration observed in Fig. 7. If the effective diffusion constant is

$$D = \frac{D_1 + 2D_2 c_2/c_1}{1 + 2c_2/c_1} = \frac{(\alpha a^2/4)\{(1/21) + [\beta/20(\beta-2\alpha)]\}}{\{1 + [2\alpha/(\beta-2\alpha)]\}}, \tag{15}$$

where $D_1 = \nu_1 a^2 e^{-E_M{}^1/kT}$ and $D_2 = \frac{1}{8}\nu_2 a^2 e^{-E_M{}^2/kT}$ where a is the interatomic distance, then in the steady state at −50°C one finds that $D = a^2\{0.02031 + 0.02163\}$ where the two numbers refer to the contribution to D from single vacancies and divacancies. Since the denominator of the above expression is approximately unity, it is clear that minor alterations in the frequency factors or the activation energies will not change the relative contributions of single vacancies and divacancies to the diffusion. Moreover, the above equation for D would lead one to expect $E_M{}^1$ (from α) as the migration energy. This is certainly not observed.

In summary the long annealing time predicted and the fact that one would expect essentially $E_M{}^1$ as the activation energy of migration indicate that simple clustering with only vacancies and divacancies mobile is not sufficient to explain Fig. 7.

This suggests that some other process exists which produces divacancies. One of the simplest schemes is

$$\begin{aligned} dc_1/dt &= -2\alpha c_1^2 - \beta c_1 c_2 - \delta c_1 c_3, \\ dc_2/dt &= +\alpha c_1^2 - \beta c_1 c_2 - \eta c_2 c_3 + 2\epsilon c_4 - \beta c_2^2, \\ dc_3/dt &= +\beta c_1 c_2 - \eta c_2 c_3 - \delta c_1 c_3, \\ dc_4/dt &= -\epsilon c_4 + \delta c_1 c_3 + \beta c_2^2, \\ dc_5/dt &= +\eta c_2 c_3, \end{aligned}$$

where we have supposed that single vacancies, divacancies, and trivacancies are all mobile and that quadrivacancies are not very stable, breaking up into pairs of divacancies. The larger clusters are nucleated by pentavacancies. The "feedback" proposed can arrange matters so that the divacancy concentration can grow with time initially and that it will remain reasonably high until the single-vacancy concentration drops to about the divacancy concentration. Note that the

divacancy concentration will only achieve reasonable values using the above model if the trivacancies are sufficiently mobile and if the quadrivacancies break up before a mobile defect strikes them.

The discussion just given concerning Fig. 7 is highly speculative and much more research is needed before any definite conclusions can be drawn concerning the behavior of clusters larger than divacancies.

1. Configuration of Quadrivacancy

The configurations of trivacancies have been discussed in detail by de Jong and Koehler. Here we consider the configuration of quadrivacancies, not only stable ones but also unstable ones and intermediate configurations. Figure 13(a) illustrates a tetrahedral quadrivacancy, (b) a rhombic, (c) a stable trivacancy attached to a single vacancy, not necessarily in the plane of the triangle (this will be called L quadrivacancy), (d) a triangular, and (e) some linear and bent quadrivacancies.

Vineyard and Gibson[20] calculated the binding energy of configuration (a) in copper and found that this is unstable. They considered two other configurations. Configuration (b) is also unstable and the corner atom in Fig. 13(b) falls into the center of the quadrivacancy. Damask, Dienes, and Weizer[17] suggested a possible trivacancy configuration (f) which has a tetrahedral shape with an atom at the center. We will call this trivacancy DDW tri. Configuration (c) is again unstable and atom (A) in Fig. 13(c) will fall into near the center of the tetrahedron. Configuration (d) and (e) are probably intermediate states leading to a stable quadrivacancy when two divacancies meet. Two other possible configurations are shown in Fig. (g) and (h).

2. Formation of Quadrivacancies and Collapsed Dislocations

Consider the process in which two divacancies meet and form a quadrivacancy. The most probable process is that a divacancy comes to one of the nearest neighbors of another divacancy forming one of the configurations

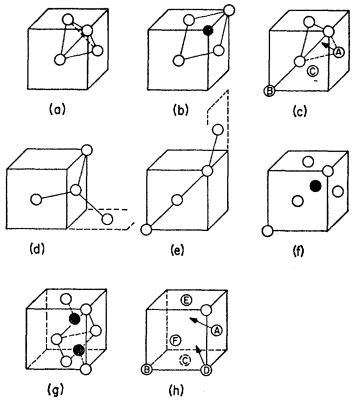

FIG. 13. Configurations of quadrivacancies.

(e) in Fig. 13. It is possible that from configuration (e) the vacancies will arrange themselves into one of the configurations (c) in Fig. 13. After configuration (c) is formed, atom A in (c) will fall into the center of the tetrahedron forming a DDW tri-attached to a vacancy B in Fig. 13(c). Following this attached vacancy B will move to the position C in Fig. 13(c), where the number of bonds between the vacancy B and the DDW tri is greater than one. Then the atom at position D in Fig. 13(h) falls near the center of the tetrahedron $CDEF$ forming configuration (g) in Fig. 13, which does not have cubic symmetry. Analogous processes will occur when a single vacancy meets a DDW tri. If another divacancy or single vacancy encounters configuration (g) in Fig. 13, then a process similar to that described above will occur. In this manner a stacking fault layer can develop on a {111} plane. This would probably be the early stage of the collapsed dislocation in a quenched specimen as observed by the elecron microscope.

V. SUMMARY

(1) The activation energy for motion of a divacancy in aluminum was interpreted to be 0.50 ± 0.04 eV.

(2) The binding energy of a divacancy in aluminum was estimated to be 0.17 ± 0.05 eV.

ACKNOWLEDGMENTS

The authors wish to express their sincere gratitude to Professor F. Seitz for his continuous interest and discussions. The authors wish to thank R. E. Hetrick and J. J. Tenicki for their assistance in this work.

[19] J. S. Koehler, F. Seitz, and J. E. Bauerle, Phys. Rev. **107**, 1499 (1957).

[20] G. H. Vineyard, Discussions Faraday Soc. **31**, 16 (1961); G. H. Vineyard and J. B. Gibson, Bull. Am. Phys. Soc. **6**, 158 (1961).